Available online at www.sciencedirect.com
SCIENCE DIRECT®
Journal of Nuclear Materials 337–339 (2005) 395–399
journal of nuclear materials
www.elsevier.com/locate/jnucmat

Modelling of heat deposition onto the Tore Supra toroidal pumped limiter

X. Bonnin *, Ph. Ghendrih, E. Tsitrone, R. Mitteau

Association EURATOM-CEA, CEA/DSM/DRFC, CEA-Cadarache, DRFC/SIPP, Bât. 513, St.-Paul-lez-Durance, cedex F-13108, France

Abstract

The new CIEL (Composantes Internes Et Limiteur) configuration of the Tore Supra tokamak has as its main plasma-facing component (PFC) a Toroidal Pumped Limiter (TPL) [P. Garin, et al., in: Proceedings of the 20th Symposium on Fusion Technology, Marseille, vol. 2, 1998, p. 1709], which must sustain the bulk of the energy leaving the plasma. Analysis of the heat deposition pattern on the TPL indicates that perpendicular heat transport may play at least as significant a role as parallel heat transport [F. Saint-Laurent et al., Nucl. Fusion 40 (2000) 1047, R. Mitteau et al., these Proceedings]. We present a new approach for modelling the heat deposited onto the TPL, which follows test 'heat packet' trajectories backwards from the TPL towards the hot plasma column. Results are compared with experimental data and trends due to plasma parameters dependencies are described. Because of ripple effects, the limiter is covered by wetted areas with long connection lengths (tens of meters), and shadowed areas with very short connection lengths (centimeters). Sharp transitions between the two are clearly seen in experiment and also reproduced in the model.

PACS: 52.40.Hf; 52.55.Fa; 52.65.Pp; 52.55.Dy
Keywords: Edge modelling; First wall; Limiter; Power deposition; Tore Supra

1. Introduction

The Toroidal Pumped Limiter (TPL) is the principal feature of the new CIEL (Composantes Internes Et Limiteur) configuration of the Tore Supra tokamak [1,2], optimized for long discharges and actively cooled. Under standard conditions, this toroidally symmetric structure is the main plasma-facing component (PFC) and must sustain most of the plasma load. It is monitored via infrared (IR) camera diagnostics [3], which show a complicated 2-D spatial distribution of the heat deposition onto the TPL, confirmed visually during a recent machine opening, dominated by strong toroidal field ripple effects. Experimental analysis, using a flux-surface averaged heat transport model [4] indicates that a large proportion of the heat (about 50%) appears to be deposited onto the TPL through cross-field transport.

We introduce in Section 2 a method for computing the heat deposition pattern onto the TPL by following 'heat packets' backwards along field lines towards the hot plasma column. A random-walk process in the directions perpendicular to the local magnetic field further modifies the 'heat packet' trajectories. The method is akin to other Monte-Carlo models of plasma edge processes, embodied in codes such as E3D [5] or

* Corresponding author. Tel.: +33 04 4225 6145; fax: +33 04 4225 4990.
E-mail address: xavier.bonnin@cea.fr (X. Bonnin).

0022-3115/$ - see front matter © 2004 Published by Elsevier B.V.
doi:10.1016/j.jnucmat.2004.09.070

EMC3-Eirene [6], but has more modest goals as it does not attempt to solve plasma transport equations, and should be viewed as a simpler alternative to more rigorous modelling. The method is ultimately aimed at predicting consequences of turbulent transport in the plasma edge. Some selected results from the method are presented in Section 3. Section 4 draws some conclusions from the existing work and provides avenues for further extensions and applications of the model.

2. Calculation method

We present a new approach for obtaining the heat deposited onto the TPL and extendable to any other PFC, which follows test 'heat packet' trajectories backwards from the PFCs towards the hot plasma column. The backward-in-time procedure is chosen as a CPU-saving measure, allowing one to concentrate only on trajectories impacting the PFC of interest. The 'heat packets' are constrained to move parallel to the magnetic field, with an additional perpendicular component having a random walk character. Different heat transport models can be represented through varying random-walk step distributions, in terms of frequency and amplitude of the perpendicular steps, both of which may vary with plasma parameters and spatial location. The relative importance of the parallel and perpendicular heat transport channels can be specified either artificially or by computing it from various physical models. The ultimate goal is to be able to compute the consequences of turbulence in the plasma edge of fusion devices in terms of heat and particle transport to plasma-facing components.

One first needs an accurate 3-D description of the magnetic field in Tore Supra, including plasma and ripple effects. The toroidal field is provided by $N = 18$ equally spaced coils, and the ripple between the coils can reach up to 7% of the field value under them [7]. We describe this rippled (vacuum) field with an axisymmetric component and the first two harmonics of the ripple frequency, i.e. $\sin(N\phi)$ and $\sin(2N\phi)$ where ϕ is the toroidal angle. The poloidal field, coming from the plasma current, the poloidal coils and induced currents in the toroidally continuous TPL, is measured by a set of magnetic probes [8]. The ripple correction to the poloidal field is computed by assuming an expansion of the plasma cross-section between the coils and enforcing analytically $\nabla \bullet \boldsymbol{B} = 0$. This yields a connection length map for the area of interest (Fig. 1). The limiter is divided into areas with long connection lengths (tens of meters), and shadowed areas with very short connection lengths (centimeters). The transition between the regions is very sharp and clearly seen in experiment. Their exact shape depends on the strengths of the toroidal magnetic field and plasma current. Within the long connection length region, one must also distinguish between field lines that contact the TPL at both ends on both sides of the plasma and traveling several times around the torus in the toroidal direction, and shorter field lines that connect the TPL to other vacuum vessel components such as the antennae or other limiting structures.

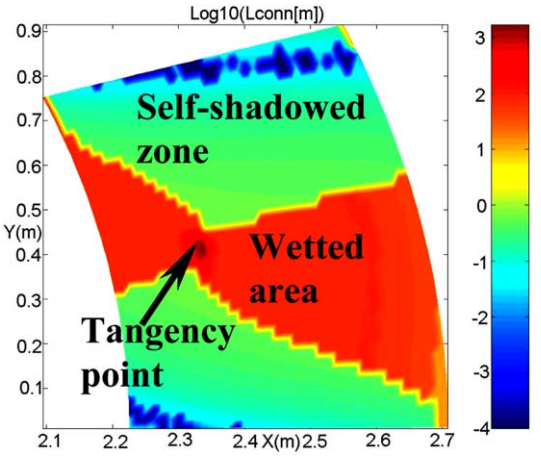

Fig. 1. Logarithmic map of connection lengths for field lines impacting a 20° sector of the Tore Supra Toroidal Pumped Limiter (TPL). One clearly sees a sharp boundary between self-shadowed areas with very short connection lengths and plasma-wetted areas where the field lines wrap around the plasma column. The precise location and shape of this boundary depends on toroidal field strength and plasma current.

The heat packet trajectories are computed in a Monte-Carlo fashion, launching from the intersections of a point mesh on the surface of interest. The mesh density and number of trajectories are user-controlled. The parallel component of the trajectories is traced using a Runge–Kutta method. In order to minimize rounding-off errors, which in our case lead to a spiraling inward of the trajectories, we ensure that each parallel step does not change the toroidal flux coordinate Ψ of the heat packet, i.e. we replace the radial component of the field line following equation

$$\delta_r/B_r = \delta_\theta/B_\theta = \delta_\phi/B_\phi \quad (1)$$

by $\delta\Psi = 0$. The distance traveled along a field line between two radial steps can either set be constant or follow some transport law dependent on local plasma parameters. Both the size and the direction distributions of the steps perpendicular to the field line can have arbitrary behaviors. After each step, parallel or perpendicular, we check whether the heat packet has impacted a wall or entered the hot plasma volume. The precise point of impact is determined and the trajectory is terminated. In the latter case, we mark this trajectory as leading to heat deposition, and add its contribution to the heat pattern.

The standard analysis [4] implies a break-up of the heat flux onto the TPL into parallel and perpendicular components:

$$\Phi = \Phi_{\parallel} \exp(-r/\lambda q) \sin\alpha + \Phi_{\perp} \exp(-r/\lambda q) \cos\alpha, \qquad (2)$$

where Φ is the heat flux, α the incidence angle of the field line (typically a few degrees), and λq is the heat decay length (of the order of a few millimeters to centimeters). Note that the decay length is a flux surface averaged quantity that only grossly parametrizes the heat transport dynamics. In general, a heat transport model would include convective and conductive components, both in the radial and parallel directions, with the convective velocity field likely to be driven in part by turbulent processes. In our formulation, the $\Phi_{\parallel}$ and $\Phi_{\perp}$ correspond to the fractions of trajectories starting with a parallel step or a radial excursion, respectively. Thus, $\Phi_{\perp}$ grows with the importance of perpendicular vs parallel transport, but in a non-trivial and model-dependent way.

The heat deposition can be punctual, when the heat packet size is considered to be zero and all its energy is dumped at the point of impact. The next step in complexity is to consider that the heat packet trajectory represents a guiding-center approximation to the plasma flow impacting the PFC surface, and to give some spatial distribution around this center to the heat packet. With gyrophase averaging, one then obtains a heat deposition pattern corresponding to a sum of elongated ellipses. These ellipses have a lateral size (perpendicular to the projection of the field line onto the PFC) of order ρ_i, and an elongation in the direction of the projection of the impacting field line of either $\rho_i/\sin\alpha$ or $\rho_i/\cos\alpha$, for parallel and perpendicular heat deposition respectively.

3. Results and analysis

Here we will consider as a first step a simple diffusive model for the trajectories. Following [9], the parallel step length $\Delta\ell$ is given by

$$\Delta\ell = \frac{-\ln(\mathrm{RND})}{2D_{\perp}/v_{th,e}\Delta r^2}, \qquad (3)$$

where RND is a random number between 0 and 1. Here, Δr, the size of the typical radial excursion, is chosen to be the ion Larmor radius. When a radial step is called for, the angle of the step in the plane perpendicular to the local magnetic field is chosen randomly. Both Eq. (3) and the angular distribution of the radial step are model-dependent. The quantity Δr itself could also, according to physical model, vary in space, for example be a function of poloidal angle, to reflect the ballooning nature of tokamak edge transport.

If we consider a model with point-like heat packets, $D_{\perp} = 1$ m^2/s, Eq. (1) only for field line tracing, and scanning the $\Phi_{\perp}$ fraction (Fig. 2), we see the plasma footprint

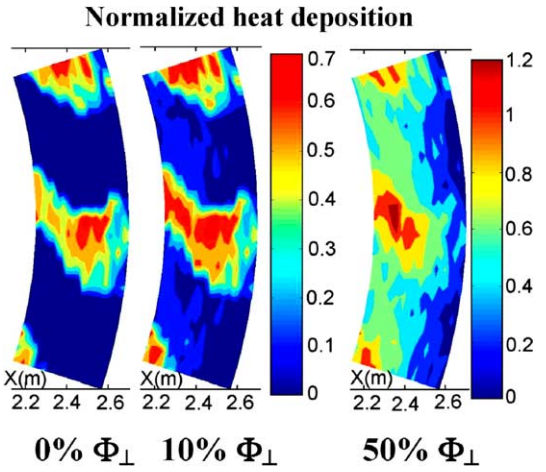

Fig. 2. Normalized heat deposition pattern predicted for a scan of the perpendicular contribution onto a 36° sector of the TPL, for $\Phi_{\perp} = 0$, 10, and 50%. As $\Phi_{\perp}$ increases, the heat deposition becomes more and more toroidally symmetric, but with a maximum at the plasma tangency point. The heat packets are assumed to be point-like, $D_{\perp} = 1$ m^2/s, and field-line tracing follows Eq. (1) only.

widening both radially and toroidally, becoming almost toroidally continuous for $\Phi_{\perp} \geqslant 50\%$. This is not a fully physical model in the sense that $\Phi_{\perp}$ and $D_{\perp}$ should not be independent of each other, but is used here for demonstration purposes. In this simplified model, the toroidal differences are all essentially due to ripple effects. A more accurate model would require separate terms in Eq. (3) for combining step sizes due to convective and conductive transport phenomena. In [3], the best match to experiment was found for $\Phi_{\perp} = 10\%$, meaning that about 50% of the heat was deposited perpendicularly. The simulated heat deposition pattern here also shows a pronounced maximum at the tangency point, which is not seen experimentally.

We have attempted to correct this latter effect by spreading the heat packet in space and refining the field line trace (enforcing $\delta\Psi = 0$). Some sample results are shown in Fig. 3 for a parabolic heat packet. Varying $D_{\perp}$ gives the profiles shown in Fig. 4. The spreading of the heat packets leads to a clear widening of the plasma footprint on the TPL, without the need for an additional $\Phi_{\perp}$ component. In a sense, the perpendicular feature of the heat deposition is now taken into account by the finite size of the heat packet. When $D_{\perp}$ is increased, we see the plasma footprint extend mostly towards the inside and the leading edge of the TPL, but its outer boundary moves much slower. There is a small amount of heat deposited at the edges of the shadowed areas, which increases with spreading parameter.

A more complex model breaks down the heat packets into components carried by ions of varying velocities, each ion velocity corresponding to a given Larmor

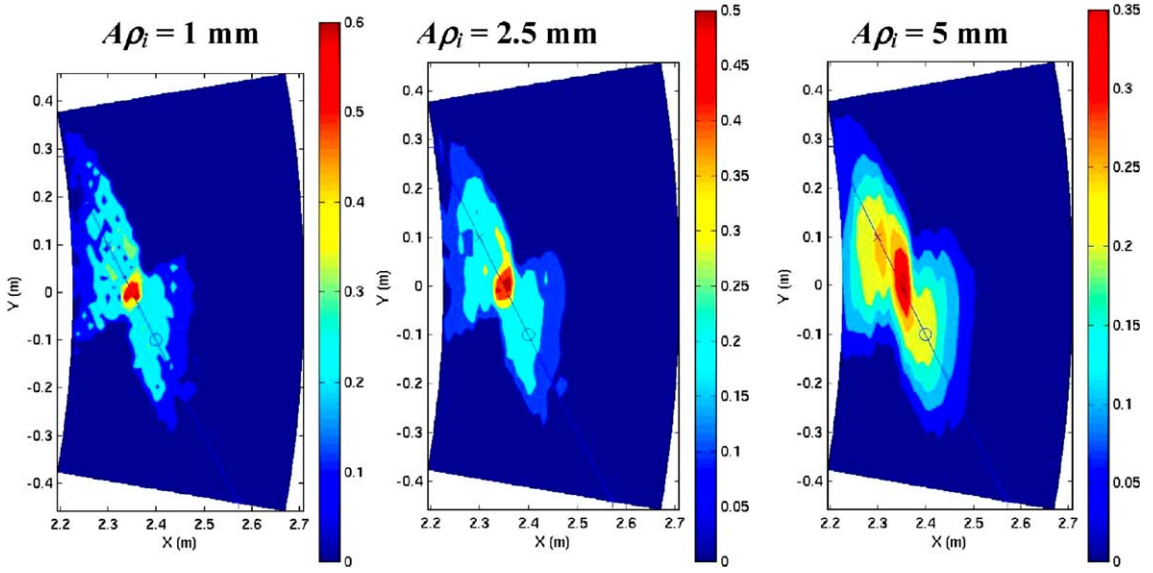

Fig. 3. Influence of parabolic heat packet size ($A\rho_i$) on normalized heat deposition pattern onto a 20° sector of the Tore Supra TPL. The case pictured has $D_\perp = 1$ m^2/s, and $\Phi_\perp = 0$. The chord along which the profiles in Fig. 4 are taken is pictured (point O corresponds to the zero abscissa in Fig. 4, with increasing abscissae going towards point X).

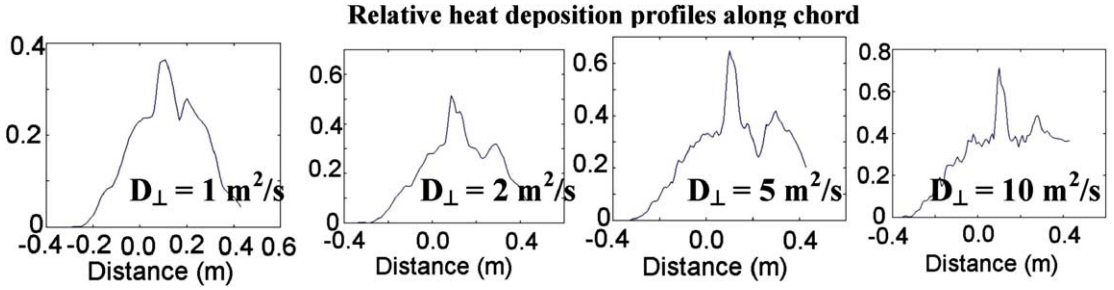

Fig. 4. Impact of $D_\perp$ on the normalized heat deposition pattern, along the diagonal featured in Fig. 3. The leading edge of the TPL is to the right of the profiles. Here, a parabolic spreading model of the heat packet is used, with heat packets of size $A\rho_i = 5$ mm and $\Phi_\perp = 0$.

radius and range of helical trajectories whose intersections with the PFC surface are then computed. Each velocity component contributes $1/2mv^2 f(v)$ where $f(v)$ is the Maxwellian distribution function for the ions. Since the velocity and the Larmor radius are linearly related, this leads to a heat distribution with a zero minimum at the guiding center. However, even with such a heat packet shape, the maximum at the tangency point remains. Another complication involves the helical ion paths about the guiding center trajectory, which lead to the particles being more likely to impact the PFC surface before rather than after their guiding center does. Further refinements including sheath effects are under consideration. Additional distinctions between convective and conductive transport as well as electron contributions of like shape, but with scale ρ_e, are also needed to complete the physics model.

4. Conclusions and outlook

We have presented some first results of simulations of the heat deposition pattern onto the Tore Supra TPL, by following Monte Carlo trajectories of heat packets connecting the limiter to the hot plasma column. This flexible method can be extended to any transport model and plasma-wall geometry. Considering the heat packets to have a finite size of order ρ_i is enough to account for a

wide plasma footprint without invoking a prompt perpendicular heat deposition component. However, reproducing the experimental shape of the heat deposition profiles will be a strong test of the precise heat packet shape. Further improvements of the model, including studies of trajectories resulting from turbulent transport models and spatial variations of the radial step distributions, are considered.

Acknowledgments

The authors would like to thank F. Saint-Laurent for providing the experimental magnetics data and guiding us though their use. Insightful discussions with S. Heuraux concerning the heat packet spreading model are gratefully acknowledged.

References

[1] P. Garin et al., in: Proceedings of the 20th Symposium on Fusion Technology, Marseille, vol. 2, 1998, p. 1709.
[2] F. Saint-Laurent et al., Nucl. Fusion 40 (2000) 1047.
[3] R. Mitteau et al., these Proceedings. doi:10.1016/j.jnucmat.2004.10.051.
[4] R. Mitteau, J.C. Vallet, A. Moal, D. Guilhem, J. Schlosser, et al., J. Nucl. Mater. 313–316 (2003) 1229.
[5] A.M. Runov, D. Reiter, S.V. Kasilov, M.F. Heyn, W. Kernbichler, Phys. Plasmas 8 (2001) 916.
[6] Y. Feng, F. Sardei, J. Kisslinger, J. Nucl. Mater. 266–269 (1999) 812.
[7] V. Basiuk, A. Bécoulet, T. Hutter, G. Martin, A.L. Pecquet, B. Saoutic, Fus. Technol. 26 (1994) 222.
[8] Ph. Moreau, P. Defrasne, E. Joffrin, F. Saint-Laurent, G. Martin, Rev. Sci. Instrum. 74 (2003) 4324.
[9] K.A. Fichthorn, W.H. Weinberg, J. Chem. Phys. 95 (1991) 1090.